

Interaction of a Peptide from the Receptor-Binding Domain of *Pseudomonas aeruginosa* Pili Strain PAK with a Cross-Reactive Antibody: Changes in Backbone Dynamics Induced by Binding[†]

A. Patricia Campbell,^{*,‡} Leo Spyropoulos,[§] Wah Y. Wong,^{||,⊥} Randall T. Irvin,^{||,⊥} and Brian D. Sykes^{§,||}

Department of Medicinal Chemistry, School of Pharmacy, University of Washington, Seattle, Washington 98195, Department of Biochemistry and Department of Medical Microbiology and Immunology, University of Alberta, Edmonton, Alberta T6G 2H7, Canada, and Protein Engineering Network of Centres of Excellence, University of Alberta, Edmonton, Alberta T6G 2S2, Canada

Received April 23, 2003; Revised Manuscript Received July 31, 2003

ABSTRACT: The C-terminal receptor-binding region of *Pseudomonas aeruginosa* pilin protein strain PAK (residues 128–144) has been the target for the design of a vaccine effective against *P. aeruginosa* infections. We have recently cloned and expressed a ¹⁵N-labeled PAK pilin peptide spanning residues 128–144 of the PAK pilin protein. The peptide exists as a major (trans) and minor (cis) species in solution, arising from isomerization around a central Ile¹³⁸–Pro¹³⁹ peptide bond. The trans isomer adopts two well-defined turns in solution, a type I β -turn spanning Asp¹³⁴–Glu–Gln–Phe¹³⁷ and a type II β -turn spanning Pro¹³⁹–Lys–Gly–Cys¹⁴². The cis isomer adopts only one well-defined type II β -turn spanning Pro¹³⁹–Lys–Gly–Cys¹⁴² but displays evidence of a less ordered turn spanning Asp¹³²–Gln–Asp–Glu¹³⁵. These turns have been implicated in cross-reactive antibody recognition. ¹⁵N NMR relaxation experiments of the ¹⁵N-labeled recombinant PAK pilin peptide in complex with an Fab fragment of a cross-reactive monoclonal antibody, PAK-13, raised against the intact PAK pilus, were performed in order to probe for changes in the mobilities and dynamics of the peptide backbone as a result of antibody binding. The major results of these studies are as follows: binding of Fab leads to the preferential ordering of the first turn over the second turn in each isomer, binding of Fab partially stabilizes peptide backbone regions undergoing slow (microsecond to millisecond) exchange-related motions, and binding of Fab leads to a greater loss in backbone conformational entropy at pH 7.2 versus pH 4.5. The biological implications of these results will be discussed in relation to the role that fast and slow backbone motions play in PAK pilin peptide immunogenicity and within the framework of developing a pilin peptide vaccine capable of conferring broad immunity across *P. aeruginosa* strains.

Pseudomonas aeruginosa is a Gram-negative rod-shaped bacterium which causes opportunistic respiratory tract infections in cancer, cystic fibrosis, and intensive care patients (1–5). The initial step in the pathogenicity of *P. aeruginosa* is adherence to the host cell via polar pili on the bacterial surface (2, 5, 6). The pili are proteinaceous filaments composed of a homologous polymer of pilin protein (5), where the semiconserved C-terminal region of the last pilin monomer in the polymer array contains the actual binding domain for adherence to the host epithelium (6–13). The seven different strains of *P. aeruginosa* so far characterized

share a common glycosphingolipid cell surface receptor (7, 14–17), where the minimal structural element is a disaccharide β GalNAc(1–4) β Gal (18) to which the C-terminal region of the pilin monomer binds.

In counteracting *P. aeruginosa* infections, an anti-adhesin vaccine has been proposed. Antibodies specific for the pilin C-terminal region can be raised with synthetic peptides and can be used to counteract infection by blocking bacterial attachment (19). Since *P. aeruginosa* exists as seven different strains, production of a cross-reactive antibody effective against all strains would be most desirable for an antibody therapeutic. It is possible to envisage such a cross-reactive antibody since all strains bind to the same receptor and display a conserved antigenic epitope (10) within the receptor-binding region (adhesintope) of the pilus (20). In fact, anti-adhesin antibodies that recognize the adhesintope inhibit pilus/fimbrial-mediated adherence of *P. aeruginosa* and *Candida albicans* to asialo-GM-1 receptors and to human buccal epithelial cell surface receptors (20). In addition, use of synthetic peptides has confirmed that the *P. aeruginosa* pilus adhesin and the *C. albicans* fimbrial adhesin possess a homologous receptor-binding domain (21).

[†] This work was funded by the Protein Engineering Network of Centres of Excellence (PENCE) and the Canadian Bacterial Diseases Network (CBDN), which are both funded by the Government of Canada.

* To whom correspondence should be addressed. Tel: (206) 685-2468. Fax: (206) 685-3252. E-mail: apc@u.washington.edu.

[‡] Department of Medicinal Chemistry, School of Pharmacy, University of Washington.

[§] Department of Biochemistry, University of Alberta.

^{||} Protein Engineering Network of Centres of Excellence, University of Alberta.

[⊥] Department of Medical Microbiology and Immunology, University of Alberta.

In an effort to understand the structural basis for cross-reactivity of the pilin monomer with antibody and receptor, we recently produced a uniformly ^{15}N -labeled immunogenic peptide spanning residues 128–144 in the C-terminal receptor-binding domain of *P. aeruginosa* pili protein strain PAK (Lys¹²⁸-Cys-Thr-Ser-Asp-Gln-Asp-Glu-Gln-Phe-Ile-Pro-Lys-Gly-Cys-Ser-Lys¹⁴⁴) using a bacterial expression system (22). The PAK(128–144) sequence is the target for the design of a synthetic peptide vaccine effective against the multiple strains of *P. aeruginosa* infection. The oxidized form of the recombinant PAK pilin peptide (containing the intramolecular disulfide bridge Cys¹²⁹–Cys¹⁴²) undergoes cis/trans isomerization of the central Ile¹³⁸–Pro¹³⁹ peptide bond. The cis/trans isomerization is manifested as a doubling of ^1H NMR¹ resonances with a trans:cis ratio of 4:1 at 5 °C (23). ^{15}N -Edited NMR structural studies have shown the trans isomer to be disordered at its N- and C-termini but ordered within the central region that encompasses two β -turns. One turn is a type I β -turn spanning residues Asp¹³⁴-Glu-Gln-Phe¹³⁷, and the other is a type II β -turn spanning residues Pro¹³⁹-Lys-Gly-Cys¹⁴² (22). The cis isomer is also disordered at its N- and C-termini but displays ordering around a type II β -turn spanning Pro¹³⁹-Lys-Gly-Cys¹⁴² (the same turn as seen in the trans isomer). NMR evidence also suggests a second β -turn spanning Asp¹³²-Gln-Asp-Glu¹³⁵ in the cis isomer, which is weakly populated in solution.

Interestingly, NMR structural studies of the intact pilin monomer from *P. aeruginosa* K122 (24) revealed the same double turn motif within the homologous disulfide-bridged C-terminal receptor-binding region of this protein (one β -turn spanning Asp¹³⁴-Asn-Lys-Tyr¹³⁷ and another spanning Pro¹³⁹-Lys-Thr-Cys¹⁴²) (25). This indicates that the double turn motif is not an artifact of working with smaller disulfide-bridged peptides but is in fact a structural motif native to the receptor-binding region of the intact pilin protein. Furthermore, the existence of a double turn motif in both the K122 pilin protein and PAK pilin peptide receptor-binding regions suggests that the double turn is conserved across all strains of *P. aeruginosa* pili, a finding that bodes well for the development of a broad strain anti-adhesin peptide vaccine.

^{15}N NMR relaxation experiments of the recombinant ^{15}N -labeled PAK pilin peptide were next undertaken to study the backbone dynamics of the receptor-binding region containing the two consecutive β -turns (26). Analysis of these relaxation data using both the model-free approach (27, 28) and spectral density mapping (29) found the type I and type II β -turns spanning residues Asp¹³⁴-Glu-Gln-Phe¹³⁷ and Pro¹³⁹-Lys-Gly-Cys¹⁴² to be the most ordered and structured regions of the trans isomer. However, slow backbone motions on the microsecond to millisecond time scale were also detected for Glu¹³⁵, Gln¹³⁶, Phe¹³⁷, Ile¹³⁸, and Lys¹⁴⁰. Thus, the two turns also appear to be a site of significant conformational exchange in the trans isomer. In agreement with these findings, ^{15}N NMR relaxation experiments of the

intact pilin monomer from *P. aeruginosa* K122 also detected microsecond to millisecond time scale motions for residues within the structurally and functionally homologous β -turns, Asp¹³⁴-Asn-Lys-Tyr¹³⁷ and Pro¹³⁹-Lys-Thr-Cys¹⁴² (24). These are intriguing results as conformational exchange has been proposed to be involved in induced-fit binding (30, 31), a mechanism which may allow Mab PAK-13 to recognize and bind pilin peptide or the intact pilus from several different strains of *P. aeruginosa*.

Having completed the structural and dynamical studies of the ^{15}N -labeled PAK pilin peptide free in solution, our current objective is to study the structure and dynamics of the ^{15}N -labeled PAK pilin peptide when these are bound to PAK-13. In a paper a few years back (32) we reported the results of ^{15}N -edited NMR structural studies of the ^{15}N -labeled PAK pilin peptide in complex with the Fab fragment of PAK-13. The results of these studies were as follows: the trans and cis isomers bound with similar affinity to the Fab, despite their different topologies; both isomers maintained the conformational integrity of their β -turns when bound to Fab; binding of Fab led to the preferential stabilization of the first turn over the second turn in each isomer; and binding of Fab led to the perturbation of resonances within regions of the trans and cis backbone that underwent microsecond to millisecond “exchange-related” motions. The discovery of microsecond to millisecond motions for residues most perturbed by Fab binding is significant insofar as these motions may play a role in induced-fit binding of the first turn to Fab PAK-13, allowing the same antibody combining site to accommodate either a trans or cis PAK pilin topology. More importantly for vaccine design, these motions may also play a role in the development of a broad-spectrum vaccine capable of generating an antibody therapeutic effective against the multiple strains of *P. aeruginosa*.

To further probe the role of the dynamics involved in antibody recognition of pilin immunogens, we have now performed ^{15}N NMR relaxation studies of the ^{15}N -labeled recombinant PAK pilin peptide in complex with Fab PAK-13 and present the results of these studies in this paper. These studies will allow an assessment of changes in the amplitude and frequencies of backbone motions of the PAK pilin peptide as a function of binding, so that changes in conformational entropy between the free and bound state may be approximated, the role of conformational exchange addressed, and possible mechanisms of conformational exchange explored. A detailed structural and dynamical picture of PAK pilin immunogenicity may ultimately provide information useful in the design of a potent synthetic peptide vaccine, immunospecific against *P. aeruginosa* infections, yet effective across the multiple strains of pilin.

MATERIALS AND METHODS

Preparation of the Recombinant ^{15}N -Labeled PAK Pilin Peptide NMR Sample. Details of the vector construction, cloning, expression, and purification of the ^{15}N -labeled PAK pilin peptide have been previously described in detail (33, 34). The sequence of the final ^{15}N -labeled recombinant peptide construct was Lys¹²⁸-Cys¹²⁹-Thr¹³⁰-Ser¹³¹-Asp¹³²-Gln¹³³-Asp¹³⁴-Glu¹³⁵-Gln¹³⁶-Phe¹³⁷-Ile¹³⁸-Pro¹³⁹-Lys¹⁴⁰-Gly¹⁴¹-Cys¹⁴²-Ser¹⁴³-Lys¹⁴⁴-Hs¹⁴⁵, where Hs¹⁴⁵ indicates an additional homoserine residue at the C-terminus, a stable product of

¹ Abbreviations: DSS, 2,2-dimethyl-2-sila-5-pentanesulfonate; ELISA, enzyme-linked immunosorbent assay; HSQC, heteronuclear single-quantum coherence; NMR, nuclear magnetic resonance spectroscopy; NOE, nuclear Overhauser effect; NOESY, 2D nuclear Overhauser effect spectroscopy; TRNOE, transferred nuclear Overhauser effect; TR-NOESY, 2D transferred nuclear Overhauser effect spectroscopy.

the cyanogen bromide cleavage of a methionine residue engineered into the end of the peptide sequence. Once isolated and purified, the recombinant peptide was oxidized to form an intramolecular disulfide bridge between residues Cys¹²⁹ and Cys¹⁴², according to the protocol outlined in ref 35.

Production of Monoclonal Antibody, Mab PAK-13, and Its Fab Fragment. Monoclonal antibody, Mab PAK-13, was prepared in mouse ascites as described previously (10, 36). The Fab fragment of PAK-13 was then produced via papain digestion of purified IgG, using the procedure outlined in ref 22.

Competitive ELISA Assays of Recombinant PAK Pilin Peptide Binding to Mab PAK-13. Competitive ELISA was carried out according to the protocol described by Wong et al. (37) in order to measure the apparent association constant (K_a) for the binding of the recombinant PAK pilin peptide to Mab PAK-13. The binding of the synthetic PAK pilin peptide to Mab PAK-13 was also measured for comparative purposes. Briefly described here, microtiter wells were coated with intact PAK pili and incubated at pH 7.2 with a solution mixture of Mab PAK-13 and recombinant peptide (or synthetic peptide) at various concentrations of peptide. The K_a for the association of peptide to PAK-13 was then calculated by the formula $K_a = 1/I_{50}$ as described by Nieto et al. (38).

Preparation of NMR Samples and Issues of pH and Temperature. Two separate peptide NMR samples were identically prepared by dissolving recombinant ¹⁵N-labeled PAK pilin peptide in 500 μ L of 90% H₂O/10% D₂O PBS buffer to a concentration of 1 mM, with DSS added as an internal chemical shift reference. The pH of the first sample was then adjusted to pH 7.2 and the pH of the second sample to pH 4.5 using NaOH and HCl solutions. The preparation of these separate peptide samples allowed all subsequent ¹⁵N NMR relaxation experiments to be performed at both pH 7.2 and pH 4.5, enabling a determination of the effects of pH on peptide backbone dynamics and antibody recognition. In addition, as the recent ¹⁵N-edited NMR structural studies of the ¹⁵N-labeled PAK pilin peptide in complex with the Fab fragment of PAK-13 had been performed at both pH 7.2 and 4.5 (32), the present dynamical study required that both pHs also be systematically investigated.

The Fab PAK-13 to be used in the titration of the two ¹⁵N-labeled PAK pilin peptide samples was prepared in the following manner. The Fab PAK-13 solution described above was dialyzed against PBS buffer, pH 7.2, and diluted 4:1 v/v in H₂O to remove excess salts, and the dialysate was lyophilized down to dryness. The powder was then dissolved in 50 μ L of H₂O to an approximate concentration of 3.5 mM, determined from an extinction coefficient at 280 nm of $\epsilon_{280} = 7.5 \times 10^7$ cm²/mol (this corresponds to an estimated OD 280 of 1.5 at a concentration of 1 mg/mL). Two separate titrations were then performed, one using the first ¹⁵N-labeled PAK pilin peptide sample prepared at pH 4.5 and one using the second peptide sample prepared at pH 7.2. Aliquots of 10–20 μ L were added to each peptide NMR sample, corresponding to 0.15 and 0.3 molar equiv of Fab/peptide. The pH was checked and readjusted to either pH 4.5 \pm 0.02 units or pH 7.20 \pm 0.02 units after each addition.

¹⁵N T_1 and T_2 and $\{^1\text{H}\}$ –¹⁵N NOE Relaxation Measurements. At each stage of the titration (0.0, 0.15, and 0.30 molar

equiv of Fab/peptide), ¹⁵N NMR relaxation experiments were carried out at 5.0 °C using the enhanced sensitivity pulsed-field gradient method (39, 40) on a Varian Inova-500 spectrometer equipped with three channels, a pulsed-field gradient triple resonance probe with an actively shielded z gradient, and a gradient amplifier unit. The pulse sequences used to record ¹⁵N T_1 and T_2 values and the steady-state heteronuclear $\{^1\text{H}\}$ –¹⁵N NOE's are from Farrow et al. (41). Relaxation delays of 11.1, 22.2, 44.4, 88.8, 177.6, 355.2, 710.4, and 1420.8 ms were used for the T_1 experiments acquired in the absence and presence of Fab. Relaxation delays of 15.6, 31.3, 46.9, 62.6, 93.4, 124.8, 156.4, and 187.2 ms were used for the T_2 experiments acquired in the absence of Fab, and delays of 16.4, 32.7, 49.1, 65.4, 81.8, 98.2, 114.5, 130.9, 147.2, 163.6, and 180.0 ms were used for the T_2 experiments acquired in the presence of 0.15 and 0.30 molar equiv of Fab. Field strengths of 6.5 and 3.8 kHz were used for ¹⁵N excitation pulses in the T_1 and T_2 experiments, respectively. WALTZ-16 decoupling (42) of ¹⁵N during acquisition was performed using a field strength of 1.2 kHz. All T_1 and T_2 experiments were obtained with 32 transients per complex point and using relaxation delays of 2 s. The $\{^1\text{H}\}$ –¹⁵N steady-state NOE was obtained by recording spectra with and without 3 s of ¹H saturation. In the case of spectra acquired without NOE, a net relaxation delay of 5 s was employed, whereas a delay of 2 s prior to 3 s of ¹H saturation was employed for spectra with NOE. The NOE experiments used a field of 6.5 kHz for the hard pulses, 1.2 kHz for WALTZ-16 decoupling, and 10.6 kHz for ¹H saturation. All NOE experiments were obtained with 64 transients per complex point. The spectral widths used for every relaxation experiment were 6000 and 970 Hz for ¹H and ¹⁵N, respectively.

Measurement of Conformational Exchange. Conformational exchange processes on 0.5–5 ms time scales were assessed at 5.0 °C and 500 MHz for the ¹⁵N-labeled PAK pilin peptide in the absence and presence of 0.3 molar equiv of Fab. These experiments used a relaxation-compensated CPMG (rc-CPMG) pulse sequence that measures ¹⁵N T_2 relaxation rates as a function of the delay between the pulses in the spin–echo pulse train, i.e., $R_2(\tau_{cp})$ (43). Two different τ_{cp} delays were used, 1 and 10 ms. Relaxation delays were identical to those employed for the T_2 experiments in the absence and presence of Fab (see above). Field strengths of 3.8 kHz were used for ¹⁵N excitation pulses. GARP decoupling (44) of ¹⁵N during acquisition was performed using a field strength of 1.0 kHz. All CPMG experiments were obtained with 32 transients per complex point and using relaxation delays of 2 s. Spectral widths were 5500 and 1115 Hz for ¹H and ¹⁵N, respectively.

Data Processing and Analysis. All 2D data sets were processed on SUN Sparc5 and Silicon Graphics Indigo2 workstations using the NMRPipe software (45). Assignment of NMR spectra was achieved with the program PIPP (46). Typically, spectra were processed in the acquisition and indirect dimension with 90° shifted sine-bell squared window functions. T_1 and T_2 values were determined by nonlinear least-squares fitting of the measured peak heights to a two-parameter exponential decay. Fitting was accomplished with the xcvfit program (executable available at the following address: <http://www.pence.ualberta.ca/~rbo/xcvfit>). Uncertainties in T_1 and T_2 values were approximated from the

nonlinear least-squares fits. The steady-state NOE values were determined from the ratio of the peak intensities obtained with and without ^1H saturation.

RESULTS

Determination of the Exchange Regime for the PAK Pilin Peptide–Fab PAK-13 Complex. The exchange regime for the PAK pilin peptide–Fab PAK-13 complex was determined using a combination of competitive ELISA experiments and chemical shift analysis. Competitive ELISA experiments performed at pH 7.2 produced a K_a of $(6.3 \pm 0.5) \times 10^6 \text{ M}^{-1}$ for the binding of the recombinant PAK pilin peptide to Mab PAK-13. For $K_a = k_1[\text{Fab}]/k_{-1}$, and assuming $k_1[\text{Fab}] = 10^8 \text{ M}^{-1} \text{ s}^{-1}$ (the diffusion-controlled on-rate), k_{-1} can be calculated to be on the order of 100 s^{-1} . Analysis of chemical shift perturbations observed for the PAK pilin peptide trans and cis resonances as a function of added Fab PAK-13 produced off-rates of similar magnitude; $k_{-1} \gg 105 \text{ s}^{-1}$ for the trans isomer, and $k_{-1} \gg 140 \text{ s}^{-1}$ for the cis isomer (32). An off-rate of $k_{-1} \gg 100 \text{ s}^{-1}$ is consistent with fast exchange on the chemical shift time scale² for both isomers, so that the ^{15}N T_1 relaxation rate and the $\{^1\text{H}\}$ – ^{15}N NOE measured for the trans and cis PAK pilin peptide resonances in the presence of antibody will be population weighted averages of their free and bound values (i.e., $R_{1\text{obs}} = P_B R_{1B} + P_F R_{1F}$). This allows a quantitative interpretation of Fab-induced changes in T_1 and NOE. However, the ^{15}N T_2 relaxation rate, R_2 , measured for the peptide resonances in the presence of antibody contains an additional exchange term [$R_{2\text{obs}} = P_B R_{2B} + P_F R_{2F} + P_B P_F(\tau)(2\pi\Delta\delta)^2$]. This exchange term has nothing to do with conformational exchange processes in either the free or bound states but is a consequence of the binding dynamic equilibrium. If a lower limit on the off-rate is taken ($k_{-1} \sim 100 \text{ s}^{-1}$), the exchange term can be expected to be of the same order of magnitude as the bound relaxation term. Thus, caution must be exercised in the quantitative interpretation of Fab-induced changes in T_2 . Nonetheless, it should be noted that no correlation was found between the size of the chemical shift perturbation experienced by a particular peptide ^{15}N nucleus and the overall Fab-induced change in T_2 measured for it [$(R_{2\text{obs}} - P_F R_{2F})$ versus $(\Delta\delta)^2$]. This suggests that exchange contributions to $T_{2\text{obs}}$ are minimal.

^{15}N T_1 and T_2 and Steady-State Heteronuclear $\{^1\text{H}\}$ – ^{15}N NOE Measurements. The 500 MHz ^{15}N T_1 and T_2 relaxation rates and steady-state heteronuclear $\{^1\text{H}\}$ – ^{15}N NOE's were measured for the trans and cis isomers of the recombinant ^{15}N -labeled PAK 128–144(Hs145) at two separate pHs (pH 4.5 and 7.2), and for three concentrations of PAK-13 Fab (0.0, 0.15, and 0.30 molar equiv of Fab). The values of these relaxation parameters are presented in Table S1 (see Supporting Information). The larger errors associated with the cis isomer parameters are a function of the smaller concentration of the cis isomer in solution, which is present at a ratio of approximately 1:4 cis:trans at 5 °C (23). Thus, at

the concentration of 1 mM peptide used, the actual concentration of cis isomer is 0.2 mM, as opposed to 0.8 mM for the trans isomer. This poor signal to noise precluded an analysis of cis isomer backbone dynamics using the model-free approach, since the nonconvergence of the T_1/T_2 ratios made calculation of a meaningful global correlation time impossible. However, a partial analysis using reduced spectral density mapping was possible.

T_1 , T_2 , and NOE of the Trans Isomer in the Absence of Fab PAK-13. Figure 1 presents the ^{15}N T_1 and T_2 and $\{^1\text{H}\}$ – ^{15}N NOE values measured at pH 7.2 (Figure 1A) and pH 4.5 (Figure 1B) for the trans isomer of the recombinant PAK pilin peptide at 0.0 (dashed line, open circles), 0.15 (thin line, gray circles), and 0.30 (thick line, black circles) molar equiv of Fab PAK-13. The ^{15}N T_1 and T_2 data acquired for the trans isomer at 0.0 molar equiv of Fab show T_1 and T_2 relaxation times that are longer for the C-terminal residues, Lys¹⁴⁴ and Hs¹⁴⁵, than for residues within the disulfide loop (residues 130–142 for pH 7.2³ and residues 129–142 for pH 4.5), suggesting that the disulfide bond imparts mobility restrictions for residues within the loop. However, even within the loop, residues do not experience a uniformity of time scales or amplitudes for their motions. For example, the T_2 times measured for Thr¹³⁰, Glu¹³⁵, Ile¹³⁸, and Lys¹⁴⁰ at pH 7.2 and Thr¹³⁰, Phe¹³⁷, Ile¹³⁸, and Lys¹⁴⁰ at pH 4.5 are considerably shorter than the T_2 times measured for other loop residues. These shortened T_2 's suggest either (1) restricted mobility (increase in local correlation time), (2) the presence of some exchange process (R_{ex}) which leads to chemical shift differences at the nitrogen on a microsecond to millisecond time scale and the appearance of enhanced transverse relaxation, or (3) anisotropic contributions caused by the alignment of the relevant NH vector along the long axis of an anisotropic diffusion tensor so that this vector reorients more slowly than others in the molecule. This third “anisotropic” explanation for the shortened T_2 's is the least likely of the three, given the continuum of intermediate to high-frequency motions that characterize small flexible peptides, like the PAK pilin peptide.

The $\{^1\text{H}\}$ – ^{15}N NOE data acquired for the trans isomer at 0.0 molar equiv of Fab (Figure 1) show maximum positive NOE values for Lys¹⁴⁰, Gly¹⁴¹, and Cys¹⁴², at both pH 7.2 and pH 4.5. Since increasing NOE values are an indication of increasing backbone ordering, this suggests that the second type II β -turn (Pro¹³⁹–Lys–Gly–Cys¹⁴²) is the most ordered region of the peptide at either pH. In contrast to the well-ordered second turn, the comparatively smaller NOE values measured at both pH 7.2 and pH 4.5 for the residues in the first type I β -turn (Asp¹³⁴–Glu–Gln–Phe¹³⁷) suggest that this turn is less ordered in the free solution peptide at either pH. Interestingly, the NOE measured for Glu¹³⁵ is significantly larger at pH 4.5 (0.24) than at pH 7.2 (0.12), whereas the NOE measured for Gln¹³³ is significantly smaller at pH 4.5 (0.13) than at pH 7.2 (0.28). Raising the pH therefore appears to lead to an increase in the ordering of the backbone around Gln¹³³ and a decrease in the ordering of the backbone around Glu¹³⁵. These changes might be associated with titration of the glutamyl side chain of Glu¹³⁵ ($\text{p}K_a \approx 4.5$).⁴

² In the limits of fast exchange on the chemical shift time scale, a single resonance is observed at a weighted average chemical shift, $\delta_{\text{obs}} = P_B \delta_B + P_F \delta_F$. The longitudinal relaxation rate ($R_1 = 1/T_1$) of this single resonance is then given by $R_{1\text{obs}} = P_B R_{1B} + P_F R_{1F}$, and the transverse relaxation rate ($R_2 = 1/T_2$) is given by $R_{2\text{obs}} = P_B R_{2B} + P_F R_{2F} + P_B P_F(\tau)(2\pi\Delta\delta)^2$, where $\tau \sim 1/k_{-1}$ and $\Delta\delta = \delta_B - \delta_F$ (47).

³ Cys¹²⁹ is not observed at pH 7.2, either due to base-catalyzed solvent exchange with the water peak or due to some other exchange mechanism, such as disulfide-bridge isomerization (see Discussion section of the paper).

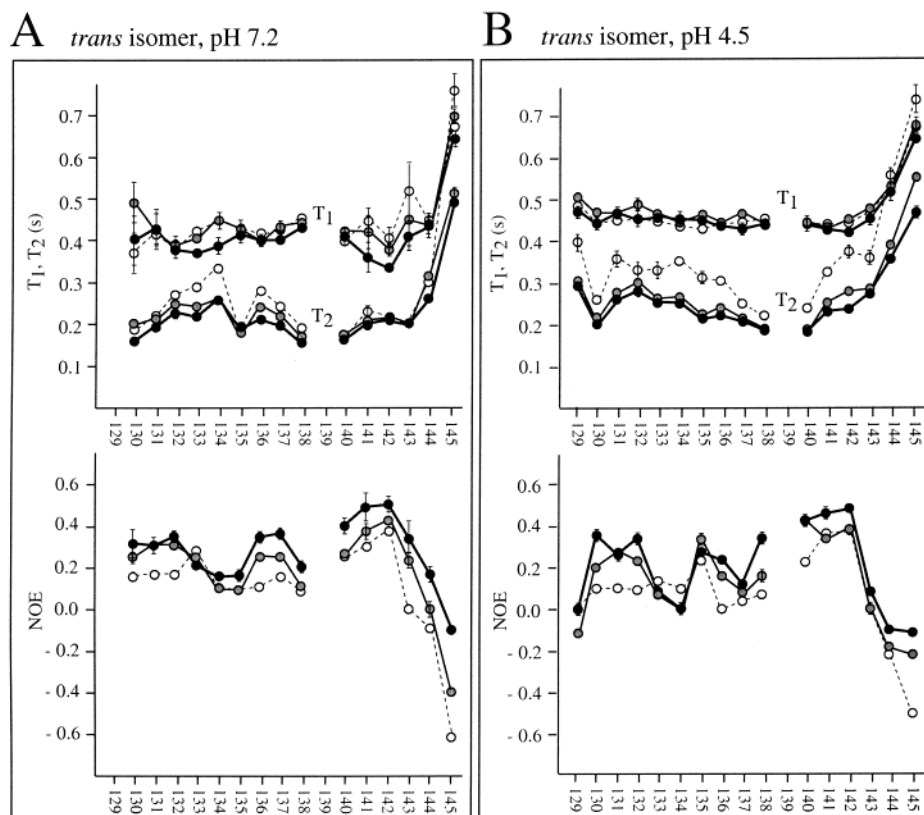


FIGURE 1: ^{15}N T_1 , T_2 , and steady-state heteronuclear $\{^1\text{H}\}-^{15}\text{N}$ NOE measured at pH 7.2 (A) and pH 4.5 (B) for the trans isomer of the recombinant PAK pilin peptide in the absence and presence of Fab PAK-13. Fab/peptide molar equivalents were 0.0 (dashed line, open circles), 0.15 (thin line, gray circles), and 0.3 (thick line, black circles). The peptide sample was 1 mM in PBS buffer and 90% $\text{H}_2\text{O}/10\%$ D_2O , 5.0 $^\circ\text{C}$. Standard deviations calculated for each parameter are plotted as error bars. Values of T_1 , T_2 , and NOE along with their associated standard deviations are listed for each trans residue in Table S1.

With the exception of Lys¹⁴⁰ in position 2 of the ordered second β -turn, the heteronuclear NOE's corresponding to residues with short T_2 's are all small valued, which implies a comparatively disordered backbone. Thus, exchange broadening (and not restricted mobility) must be the source of the enhanced transverse relaxation rates observed for these residues. Exchange broadening must also account for the shorter T_2 's measured at pH 7.2 versus pH 4.5, especially as the T_1 's and heteronuclear NOE's are roughly comparable at either pH. For example, the T_2 of Lys¹⁴⁰ is 160 ms at pH 7.2 and 240 ms at pH 4.5, whereas the NOE for this residue is the same within error at pH 7.2 versus pH 4.5 (0.25 versus 0.23, respectively). The increased exchange broadening observed at pH 7.2 could result from either increased rates of specific conformational exchange mechanisms within the trans isomer or increased rates of base-catalyzed solvent exchange with the water peak (48).

It is worth noting that the turn residue Glu¹³⁵ displays a significantly decreased T_2 at higher pH (310 ms at pH 4.5 versus 200 ms at pH 7.5). This pH dependence of Glu¹³⁵ T_2 tracks the pH dependence of Glu¹³⁵ NOE, for which increased ordering at pH 4.5 was earlier suggested. While this may reflect a more stable type I β -turn (Asp¹³⁴-Glu-Gln-Phe¹³⁷) at pH 4.5, it may also reflect a more stably bound water

molecule at Glu¹³⁵, with a longer residency time at pH 4.5. Exposed amide and carbonyl groups of β -turns are often solvated, with the water molecule occasionally forming a bridge between residues in the turn (49). Exchange of these bound water molecules with the bulk solvent has been observed to result in increased ^{15}N T_2 relaxation rates at physiological pH (50). Thus, the shortened T_2 and smaller NOE observed for Glu¹³⁵ at pH 7.2 could result from a bound water molecule that experiences an increased rate of exchange and a shorter residency time as the glutamyl side chain is titrated to its unprotonated state.

T_1 , T_2 , and NOE of the Trans Isomer in the Presence of Fab PAK-13. The ^{15}N T_1 and T_2 data acquired for the trans isomer at 0.15 and 0.30 molar equiv of Fab PAK-13 (Figure 1) show that the T_1 and T_2 times for residues within the disulfide loop region (and at the C-terminus) shorten in the presence of Fab. This is consistent with an overall increase in the correlation time of the bound trans isomer. For example, the averaged T_2 values for residues 129–142 at pH 7.2 are 240 ms in the absence of Fab (0.0 molar equiv) and 200 ms in the presence of Fab (0.30 molar equiv), representing an average decrease of 40 ms. The corresponding T_2 values at pH 4.5 are 310 ms in the absence and 230 ms in the presence of Fab, representing an average decrease of 80 ms.

Decreases in T_2 can be related to increases in local correlation time (τ_c) as well as to increases in the contribution of exchange broadening (R_{ex}) to T_2 . Thus, if R_{ex} contributions to T_2 were to decrease in the presence of Fab (due to the

⁴ A ^1H NMR-monitored pH titration of the synthetic version of the PAK pilin peptide showed titration of the backbone amide resonance of Glu¹³⁵ from 8.25 ppm at pH 4 to 8.48 ppm at pH 8, with a pK_a of approximately 4.5. No other residues displayed significant chemical shifts within this pH range.

stabilization of microsecond to millisecond exchange-related motions), then the T_2 decreases caused by τ_c increases would be minimized. This appears to be the situation for the PAK pilin peptide, where those residues associated with exchange broadening are also the ones associated with the smallest decreases in T_2 in the presence of Fab. However, these slow motions are not completely stabilized in the presence of Fab, as the existence of shortened T_2 's for select residues in the presence of Fab (Glu¹³⁵ T_2 at pH 7.2, for example) provides evidence that exchange broadening persists in the bound state.

The $\{^1\text{H}\}-^{15}\text{N}$ NOE's acquired for the trans isomer at 0.15 and 0.30 molar equiv of Fab PAK-13 (Figure 1) show significant increases for many residues in the presence of Fab. At pH 7.2, these residues include Thr¹³⁰, Ser¹³¹, and Asp¹³² on the N-terminal side of the first turn, Gln¹³⁶ and Phe¹³⁷ within the first turn, Lys¹⁴⁰ and Gly¹⁴¹ within the second turn, and Ser¹⁴³, Lys¹⁴⁴, and His¹⁴⁵ at the C-terminus. At pH 4.5, these residues include Thr¹³⁰, Ser¹³¹, and Asp¹³² on the N-terminal side of the first turn, Gln¹³⁶ in the first turn, Ile¹³⁸ between turns, Lys¹⁴⁰ in the second turn, and His¹⁴⁵ at the C-terminus. Thus, more residues are ordered by Fab binding at the higher pH. Despite these pH-related differences, binding of Fab at both pH 7.2 and pH 4.5 appears to order three distinct regions of the sequence: residues 130–132 upstream of the two turns, residues 136–141 within the two turns, and C-terminal residues just outside of the disulfide-bridged region. Separating regions one and two are Gln¹³³ and Asp¹³⁴, for which no increases in NOE values are observed in the presence of Fab at either pH 7.2 or pH 4.5.

The NMR solution structure of the trans isomer of the synthetic PAK pilin peptide (35) shows that the backbones and side chains of residues Gln¹³⁶, Phe¹³⁷, Ile¹³⁸, Pro¹³⁹, Lys¹⁴⁰, Ser¹⁴³, and Lys¹⁴⁴ are located on the top face of the molecule. Thus, the second half of the first turn (Gln¹³⁶–Phe¹³⁷), the hydrophobic pocket (Phe¹³⁷, Ile¹³⁸, and Pro¹³⁹), the first half of the second turn (Pro¹³⁹–Lys¹⁴⁰), and the C-terminus (Ser¹⁴³ and Lys¹⁴⁴) comprise a contiguous surface for interaction with antibody. The NMR solution structure of the trans isomer also shows that the backbones and side chains of residues Thr¹³⁰, Ser¹³¹, Asp¹³², Gln¹³³, and Asp¹³⁴ are located on the bottom face of the molecule, away from the proposed binding surface. Thus, the significant increases in the heteronuclear NOE's observed for Thr¹³⁰, Ser¹³¹, and Asp¹³² must be related to an overall "tightening" of the peptide, as opposed to direct contact with Fab. As Thr¹³⁰ is just downstream of Cys¹²⁹, a decrease in the motional flexibility of the Cys¹²⁹–Cys¹⁴² disulfide bond as the second turn is bound (Cys¹⁴² is in position 4 of this turn) may contribute to the increased ordering of Thr¹³⁰. Interestingly, the side chains of Thr¹³⁰ and Ser¹³¹ also point inward toward the hydrophobic pocket of the peptide. Thus, a tightening of the hydrophobic pocket might additionally contribute to the ordering of these residues. By contrast, the backbone and side chains of Gln¹³³ and Asp¹³⁴ are looped out toward the bottom surface of the peptide. Their relative detachment from the rest of the peptide may explain why no increases in ordering were observed for these residues in the presence of Fab.

If the $\{^1\text{H}\}-^{15}\text{N}$ NOE's for the turns alone are considered, it can be seen that the first turn residues undergo greater

ordering than the second turn residues in the presence of Fab, regardless of pH. This is in agreement with the results of our ^{15}N -edited TRNOESY studies published earlier (32), which showed TRNOE enhancements only for first turn residues. In the same paper, backbone coupling constants were used to estimate turn populations in the absence and presence of Fab. Values were obtained of 56% and 74% for the first turn in the absence and presence of Fab, respectively, and 70% and 68% for the second turn in the absence and presence of Fab, respectively (32). Thus, binding of Fab PAK-13 leads to preferential stabilization of the first turn over the second turn in the trans isomer.

T₁, T₂, and NOE of the Cis Isomer in the Absence and Presence of Fab PAK-13. The ^{15}N T_1 and T_2 data acquired for the cis isomer at 0.0 molar equiv of Fab PAK-13 (see Table S1, data not plotted) suggest that the disulfide bond imparts mobility restrictions for residues within the disulfide loop, as earlier postulated for the trans isomer. Residues within the loop region that exhibit shortened T_2 times are Thr¹³⁰, Asp¹³², Phe¹³⁷, and Gly¹⁴¹ at pH 7.2 and Thr¹³⁰, Asp¹³², Phe¹³⁷, and Gly¹⁴¹ at pH 4.5. However, these T_2 times are much shorter than the T_2 times observed for the same residues in the trans isomer. In addition, the collection of residues that display shortened T_2 times is different for the cis isomer (Thr¹³⁰, Asp¹³², Phe¹³⁷, and Gly¹⁴¹) than for the trans isomer (Thr¹³⁰, Glu¹³⁵, Phe¹³⁷, Ile¹³⁸, and Lys¹⁴⁰), suggesting that different conformational exchange mechanisms exist in each isomer.

The ^{15}N T_2 data acquired for the cis isomer at 0.15 and 0.30 molar equiv of Fab PAK-13 (Table S1) show that the T_2 times for residues within the disulfide loop region shorten in the presence of increasing Fab. As previously suggested for the trans isomer, this shortening is consistent with an overall increase in the correlation time of the bound cis isomer.

The $\{^1\text{H}\}-^{15}\text{N}$ NOE data acquired for the cis isomer at 0.0 molar equiv of Fab (Table S1) show maximum positive NOE values for Lys¹⁴⁰, Gly¹⁴¹, and Cys¹⁴² at both pH 7.2 and pH 4.5, implying that the second turn is the most ordered region of the peptide at both pH 7.2 and pH 4.5 (as seen with the trans isomer). Asp¹³² also displays a relatively large NOE, suggesting increased ordering of the backbone around this residue as well. Previous heteronuclear NMR experiments of the recombinant PAK pilin peptide at pH 4.5 indicated the presence of a turn spanning Asp¹³²–Gln–Asp–Glu¹³⁵ in the cis isomer, which was less ordered and less well conformationally defined than the second type II turn (34).

The $\{^1\text{H}\}-^{15}\text{N}$ NOE data acquired for the cis isomer at 0.15 and 0.30 molar equiv of Fab PAK-13 (Table S1) show significant increases for several residues in the presence of Fab. At pH 7.2, these residues include Ser¹³¹, Asp¹³², and Asp¹³⁴, located in or near the putative first turn in the cis isomer (Asp¹³²–Gln–Asp–Glu¹³⁵). These NOE data suggest that the first turn in the cis isomer is ordered by Fab binding, in agreement with the results of our ^{15}N -edited TRNOESY studies (32) that showed TRNOE enhancements for Glu¹³⁵ in the first turn. Thus, as with the trans isomer, binding of Fab to the cis isomer appears to lead to preferential ordering of the first turn over the second turn.

Model-Free Analysis of the Trans Isomer: Effects of Fab Binding. The backbone dynamics of the trans isomer of the

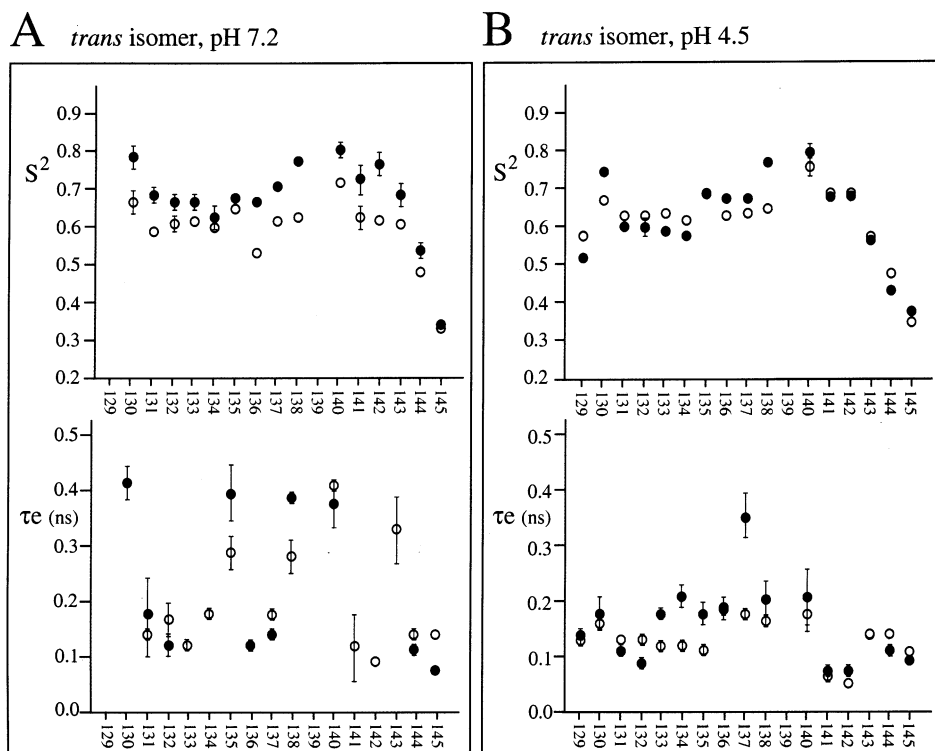


FIGURE 2: Order parameters, S^2 , and internal correlation times, τ_c , calculated from relaxation data measured at pH 7.2 (A) and pH 4.5 (B) for the trans isomer of the recombinant PAK pilin peptide in the absence (open circles) and presence (black circles) of 0.3 molar equiv of Fab PAK-13. Relaxation data were fitted to the single time scale form of the spectral density function, using only S^2 and τ_c variables. Standard deviations calculated for each parameter are plotted as error bars. Values of S^2 and τ_c along with their associated standard deviations are listed for each trans residue in Table S2.

recombinant PAK pilin peptide in the presence and absence of Fab PAK-13 were first analyzed using the model-free approach of Lipari and Szabo (27, 28). The first step in this analysis involved obtaining an estimate for the value of the global correlation time, τ_c , using T_1/T_2 ratios. The poor signal to noise associated with the cis isomer precluded such an analysis, since the nonconvergence of the T_1/T_2 ratios made calculation of a meaningful τ_c impossible. However, τ_c 's were readily calculated for the free and bound trans isomer (0.0 and 0.30 molar equiv of Fab), at both pH 4.5 and pH 7.2, using residues with backbone nitrogens within the specified threshold of one standard deviation from the mean. Residues with T_1/T_2 ratios greater than one standard deviation from the mean included Thr¹³⁰, Glu¹³⁵, Ile¹³⁸, and Lys¹⁴⁰ at pH 7.2 and Thr¹³⁰, Phe¹³⁷, Ile¹³⁸, and Lys¹⁴⁰ at pH 4.5 and were excluded from the determination of τ_c , as the relaxation of these residues was considered to be more appropriately modeled with R_{ex} contributions, which would lead to an effective decrease in the measured T_2 (50).

Using this methodology, the global optimum τ_c 's for the free and bound trans isomer were determined. Upon complexation at pH 4.5, τ_c was found to increase from $\tau_c(\text{free}) = 2.3 \pm 0.4$ ns to $\tau_c(\text{bound}) = 3.7 \pm 0.3$ ns, consistent with the different molecular masses of the free peptide (1.5 kDa) and the peptide–Fab complex (50 kDa). Upon complexation at pH 7.2, however, the τ_c values did not significantly change [$\tau_c(\text{free}) = 4.5 \pm 0.8$ ns and $\tau_c(\text{bound}) = 4.3 \pm 0.5$ ns], which may be a reflection of a looser free solution structure that becomes more compact upon binding. Interestingly, the $\tau_c(\text{bound})$ values for pH 7.2 and 4.5 are the same within error, suggesting that the ordering or “compactness” of the bound trans isomer is similar at both pHs.

Once these global τ_c 's were determined, they were used to fit the relaxation data to a single time scale form of the spectral density function, and the model-free parameters S^2 and τ_c were calculated for all backbone amide N–H bond vectors in the free and bound trans isomer at pH 7.2 and 4.5. The S^2 and τ_c values are presented in Table S2. A comparison of these values in the absence of Fab shows that the average S^2 and τ_c values for residues 129–142 are 5% smaller and 62% larger, respectively, at the higher pH. Thus, the trans isomer at pH 7.2 is slightly more disordered, with internal motions of greater rate and amplitude than those observed at pH 4.5. This agrees with the longer global optimum τ_c calculated at pH 7.2 and the appearance of increased exchange broadening at pH 7.2.

Figure 2 plots the S^2 and τ_c values for the trans isomer at pH 7.2 (Figure 2A) and pH 4.5 (Figure 2B) in the absence (open circles) and presence (black circles) of 0.30 molar equiv of Fab PAK-13. The S^2 values plotted for pH 7.2 show significant increases (≥ 0.08 S^2 unit) in ordering for Thr¹³⁰ and Ser¹³¹ near the disulfide bridge, Gln¹³⁶ and Phe¹³⁷ in the first turn, Ile¹³⁸ between the turns, and Lys¹⁴⁰, Gly¹⁴¹, and Cys¹⁴² in the second turn. These increases imply partial immobilization of the second half of the first turn (Gln¹³⁶–Phe¹³⁷), the hydrophobic pocket (Phe¹³⁷, Ile¹³⁸ and Pro¹³⁹), the second turn (Pro¹³⁹–Lys–Gly–Cys¹⁴²), and the disulfide bridge (Cys¹²⁹–Cys¹⁴²), structural elements all presented on the top half of the solution structure of the PAK pilin peptide (35). However, partial immobilization does not mean an absence of internal motions in the bound state. The τ_c values plotted for the trans isomer at pH 7.2 show that the free and bound states both experience significant internal motions on the picosecond to nanosecond time scale. This is especially

true for the residues associated with exchange-related microsecond to millisecond time scale motions, as these residues display τ_e values greater than 30 ps in the bound state.

The S^2 values plotted for pH 4.5 (Figure 2B) show smaller increases in the presence of Fab. Only residues Thr¹³⁰ and Ile¹³⁸ show significant increases in ordering; residues Gln¹³⁶ and Phe¹³⁷ in the first turn show only small increases in ordering. These results imply that partial immobilization occurs only around Thr¹³⁰, Ile¹³⁸, and the second half of the first turn (Gln¹³⁶-Phe¹³⁷). Thus, while the antibody may be recognizing the same binding surface on the trans isomer, it appears to be inducing less order at pH 4.5, possibly because the free peptide is already partially "preordered for binding" at the lower pH.

To examine if exchange-related motions on the microsecond to millisecond time scale are stabilized by antibody binding, the parameter R_{ex} was added in the calculation of S^2 and τ_e using the one time scale spectral density function (51). These S^2 , τ_e , and R_{ex} values are included in Table S2 for only those residues where better or equally good fits were obtained on the basis of a χ^2 calculation. Unfortunately, the absence of a well-defined τ_e (free) for the trans isomer at pH 7.2 precluded quantitative analysis of free versus bound R_{ex} values. Thankfully, well-defined τ_e (free) and τ_e (bound) values at pH 4.5 allowed quantitative R_{ex} analysis at the lower pH, for which a significant decrease for Ile¹³⁸ in the presence of Fab was observed [R_{ex} (free) = 1.54 ± 0.23 s⁻¹ at 0.0 molar equiv of Fab; R_{ex} (bound) = 1.11 ± 0.15 s⁻¹ at 0.3 molar equiv of Fab]. Thus, binding of Fab appears to lead to the stabilization of exchange-related motions around residue Ile¹³⁸, at least at pH 4.5.

Reduced Spectral Density Mapping of the Trans and Cis Isomers: Effects of Fab Binding. Model-free analysis often provides a means of assessing the contributions of internal motions and conformational exchange to the spin relaxation of globular proteins in solution. However, there are limitations that arise from inherent assumptions. The overall molecular reorientation must be isotropic and independent from fast internal motions, whose contributions to relaxation are negligible ($\tau_c \gg \tau_e$). These assumptions do not necessarily hold for small flexible peptides in solution, especially at temperatures greater than 5 °C, above which the concept of a global τ_c is suspect due to a lack of regular secondary structure. An alternative relaxation analysis approach for characterizing molecular dynamics at multiple temperatures is provided by spectral density mapping (52, 53), which has the advantage that it makes no assumptions about the separability of the time scales between the motions and allows the possibility of sizable contributions to relaxation from high-frequency motions. Moreover, this methodology is analytic and independent of error estimates, which allows relaxation data with poor signal to noise to be interpreted (as is the case with the cis isomer of the PAK pilin peptide).

In general, $J(0)$ is proportional to the local correlation time of the backbone nitrogen (52). Thus, it is possible to interpret temperature effects on the basis of changes in local correlation times. However, this interpretation is valid only in the absence of conformational exchange phenomena, which can lead to shortening of T_2 times and, therefore, larger values of $J(0)$. In certain cases, conformational exchange phenomena can contribute significantly more to the value of $J(0)$ than

the local correlation time (54). The contribution of slow motions (microsecond to millisecond) to $J(0)$ must therefore be carefully scrutinized.

The $J(\omega)$ spectral density values, $J(0)$, $J(\omega_N)$, and $J(\omega_H)$, were calculated from the relaxation data measured for the free and bound (0.0 and 0.30 molar equiv of Fab PAK-13) trans and cis isomers of the recombinant PAK pilin peptide at pH 7.2 and 4.5 (see Table S3). Figure 3 plots the $J(0)$ values for the trans isomer of the recombinant PAK pilin peptide at pH 7.2 (Figure 3A) and pH 4.5 (Figure 3B). In the absence of Fab (open circles), the trans isomer displays the largest $J(0)$ values for Thr¹³⁰, Glu¹³⁵, Ile¹³⁸, Lys¹⁴⁰, and Ser¹⁴³ at pH 7.2 and Thr¹³⁰, Phe¹³⁷, Ile¹³⁸, and Lys¹⁴⁰ at pH 4.5, consistent with the low T_2 values measured for these residues, and the need to include R_{ex} terms in the modeling of their relaxation. The smallest $J(0)$ values are associated with Lys¹⁴⁴ and His¹⁴⁵ at both pHs, consistent with the increased short local τ_c 's for residues at the mobile C-terminus.

$J(0)$ values calculated for the trans isomer are observed to increase in the presence of 0.30 molar equiv of Fab (black circles). For example, $J(0)_{av}$ for residues 129–142 increases from 0.97 to 1.19 ns rad⁻¹ at pH 7.2 and from 0.65 to 1.10 ns rad⁻¹ at pH 4.5. At pH 4.5, these increases are relatively uniform across the sequence (with the exception of Glu¹³⁵).⁵ However, at pH 7.2, these increases are limited to residues 130–134 and 136–138 in the sequence. As the $J(0)$ values for Glu¹³⁵ and Lys¹⁴⁰ appear to be dominated by the contribution of the R_{ex} exchange term at pH 7.2, the absence of significant increases for these residues suggests that R_{ex} contributions to $J(0)$ are decreasing as a function of increasing Fab; i.e., the binding of Fab is stabilizing exchange-related motions around Glu¹³⁵ and Lys¹⁴⁰. On the other hand, where $J(0)$ is not dominated by R_{ex} , the absence of increases in $J(0)$ with increasing Fab suggests that local τ_c 's are not significantly changing. This appears to be the case for residues Gly¹⁴¹, Cys¹⁴², and Ser¹⁴³ within or near the second turn. The absence of significant increases in the local τ_c 's for these residues in the presence of Fab is in agreement with the notion of a well-ordered second turn in the free solution state of the trans isomer, which does not undergo significant further ordering in the bound state.

Significant differences are observed between $J(0)$ values calculated at pH 7.2 versus pH 4.5. The averaged $J(0)$ values calculated for all residues in the free trans isomer at pH 7.2 are approximately 40% larger than the averaged $J(0)$ values calculated at pH 4.5, reflecting either an increased rate of solvent exchange at the higher pH or the "looseness" of the free solution structure which could be undergoing various forms of conformational exchange. However, the single most striking difference between the two pHs is the size of the $J(0)$ value calculated for Glu¹³⁵ at pH 7.2 (1.21 ns rad⁻¹ at pH 7.2 versus 0.62 ns rad⁻¹ at pH 4.5). This large $J(0)$ value reflects the short T_2 measured for Glu¹³⁵ at pH 7.2, for which a possible pH-dependent bound water mechanism has already been discussed.

Figure 3 also plots the $J(0)$ values for the cis isomer of the recombinant PAK pilin peptide at pH 7.2 (Figure 3A)

⁵ At pH 4.5, the $J(0)$ of Glu¹³⁵ increases appreciably in the presence of Fab. This may reflect either an increase in R_{ex} or an increase in the local τ_c for this residue in the bound state.

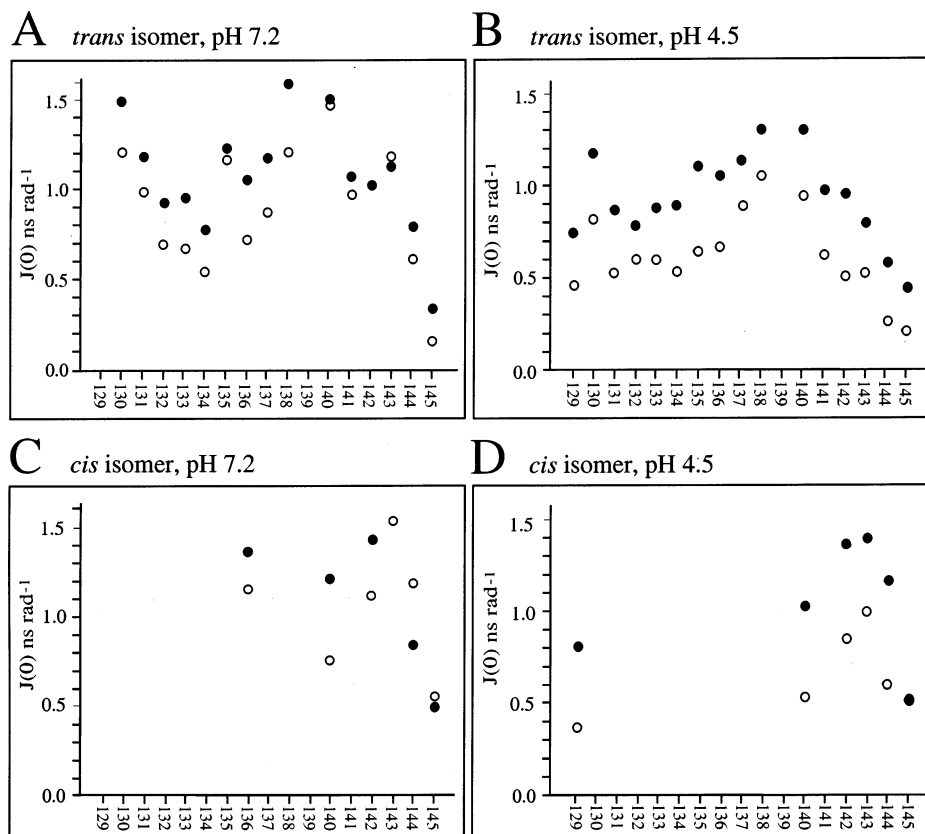


FIGURE 3: $J(0)$ spectral density values calculated from relaxation data measured at pH 7.2 (A) and pH 4.5 (B) for the trans (top panels) and cis (bottom panels) isomers of the recombinant PAK pilin peptide in the absence (open circles) and presence (black circles) of 0.3 molar equiv of Fab PAK-13. Values of $J(0)$, $J(\omega_N)$, and $J(\omega_H)$ are listed for each trans and cis residue in Table S3.

and pH 4.5 (Figure 3B). In the interest of scale and visual clarity, only select cis residues are plotted, for which reasonably small and accurate $J(0)$ values could be calculated (<2 ns rad⁻¹). These smaller $J(0)$'s are presumably not dominated by R_{ex} . Even so, $J(0)$ values are larger at pH 7.2 versus pH 4.5. As with the trans isomer, this may reflect an increased rate of either solvent or conformational exchange in the cis isomer at the higher pH. In the presence of Fab (black circles), $J(0)$ values for these select cis residues are observed to increase at both pHs, which probably reflects increases in local τ_c . Although few residues are plotted for the cis isomer and standard deviations are large, the increases in $J(0)$ for residues in the second turn and C-terminus still show that this region is bound and partially immobilized by the antibody. Unfortunately, meaningful $J(0)$ values for first turn residues in the cis isomer cannot be extracted.

Measurement of Conformational Exchange. Our analysis of T_2 relaxation data using both model-free formalism and spectral density mapping suggests a stabilization of microsecond to millisecond exchange-related motions in the trans isomer of the PAK pilin peptide when it is bound to Fab. To provide a more direct assessment of exchange-related motions in the free and bound state, we used a relaxation-compensated CPMG (rc-CPMG) pulse sequence which detects chemical or conformational exchange processes on 0.5–5 ms time scales (43).

Figure 4 shows $\Delta R_2(\tau_{cp}) = R_2(10 \text{ ms}) - R_2(1 \text{ ms})$ plotted for each residue of the trans isomer of the recombinant PAK pilin peptide in the absence and presence of 0.3 molar equiv of Fab PAK-13, pH 4.5, at 5 °C. $\Delta R_2(\tau_{cp})$ and $R_2(\tau_{cp})$ values are also given in Table S4. If exchange processes exist on

trans isomer, pH 4.5

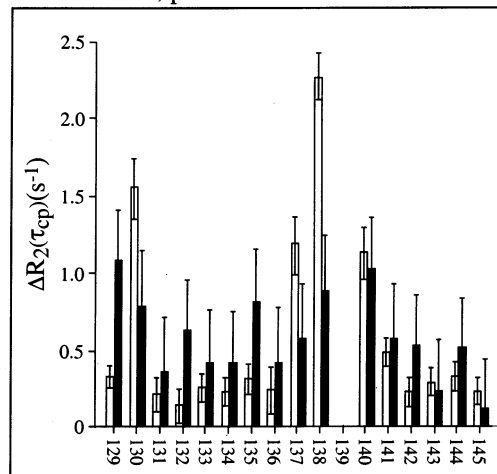


FIGURE 4: Conformational exchange at pH 4.5, calculated as $\Delta R_2(\tau_{cp}) = R_2(10 \text{ ms}) - R_2(1 \text{ ms})$, is plotted for each residue of the trans isomer of the recombinant PAK pilin peptide in the absence (open bars) and presence (black bars) of 0.3 molar equiv of Fab PAK-13. The peptide sample was 1 mM in PBS buffer, pH 4.5, and 90% H₂O/10% D₂O, 5.0 °C. Error bars represent the propagated standard deviations from the original T_2 measurements. Values of ^{15}N $T_2(10 \text{ ms})$, $R_2(1 \text{ ms})$, $T_2(1 \text{ ms})$, and $R_2(10 \text{ ms})$, along with their associated standard deviations, are listed for each trans residue in Table S4.

time scales commensurate with τ_{cp} , these processes should contribute to faster R_2 rates as τ_{cp} is increased; i.e., $R_2(10 \text{ ms}) > R_2(1 \text{ ms})$, or $\Delta R_2(\tau_{cp}) > 0$. According to Figure 4, positive $\Delta R_2(\tau_{cp})$ values larger than the mean were measured for Thr¹³⁰ ($1.56 \pm 0.21 \text{ s}^{-1}$), Phe¹²⁷ ($1.18 \pm 0.18 \text{ s}^{-1}$), and

Lys¹⁴⁰ ($2.27 \pm 0.15 \text{ s}^{-1}$) in the absence of Fab. However, these values are reduced in the presence of 0.3 molar equiv of Fab to 0.78 ± 0.39 , 0.56 ± 0.37 , and $0.87 \pm 0.32 \text{ s}^{-1}$, respectively. This suggests that Thr¹³⁰, Phe¹²⁷, and Lys¹⁴⁰ experience slow 0.5–5 ms time scale motions in the free solution state PAK pilin peptide but that these motions are quenched upon binding to Fab. In addition, the absence of significant 0.5–5 ms time scale processes in the presence of Fab suggests that chemical exchange between the free and Fab-bound state is on a time scale faster than those sampled by the rc-CPMG experiment. This is in agreement with our calculation of an off-rate of $k_{-1} \gg 100 \text{ s}^{-1}$.

DISCUSSION AND CONCLUSIONS

¹⁵N T_1 and T_2 relaxation rates and steady-state heteronuclear {¹H}–¹⁵N NOE's were measured for the ¹⁵N-labeled recombinant PAK pilin peptide in the absence and presence of a Fab fragment from monoclonal antibody PAK-13. These parameters were analyzed using both the model-free formalism and the reduced spectral density mapping approach. Exchange processes on 0.5–5 ms time scales were also assessed for the PAK pilin peptide in the absence and presence of Fab using a relaxation-compensated CPMG experiment. The results of these studies invite discussion of several key issues which include possible conformational exchange mechanisms in the trans and cis isomers of the PAK pilin peptide, the effect of pH on these exchange mechanisms, and the role of conformational exchange in induced-fit binding of antibody.

Possible Conformational Exchange Mechanisms in the Trans Isomer of the PAK Pilin Peptide. In the trans isomer, slow exchange-related motions were detected for Thr¹³⁰, at pH 7.2 and at pH 4.5. These motions could result from isomerization of chirality of the neighboring Cys¹²⁹–Cys¹⁴² disulfide bond. Disulfide bond isomerization has been observed in BPTI as a doubling of resonances in the ¹⁵N-edited HSQC spectrum of this protein (55) and has been detected in ¹⁵N relaxation analysis of the C5 domain of the human type VI collagen $\alpha 3$ chain (56) and the disulfide-bridged ω -conotoxin MVIIA polypeptide (57). According to a model representation of the two different disulfide bond arrangements in the major and minor conformations of BPTI (55), isomerization occurs as a result of a -120° rotation around the C α –C β bond of one of the cysteines. While this places the H β protons of one of the cysteines into two possible arrangements, it leaves the H β protons of the other cysteine in the same position in both isomers. A similar situation appears to be the case for the PAK pilin peptide. Close examination of the ¹⁵N-edited NOESY HSQC spectrum of the recombinant PAK pilin peptide in the absence of Fab PAK-13 (32) shows a doubling of the ¹⁵N, NH, H α (F2, F1, F3) cross-peak for Cys¹²⁹ for the trans isomer,⁶ implying that the C α –C β bond of Cys¹²⁹ is undergoing conformational exchange so as to place the H α into two chemically different environments. Interestingly, the doubling of Cys¹²⁹ H α resonances is still observed in the NOESY HSQC in the presence of Fab PAK-13,⁷ suggesting that

isomerization of the Cys¹²⁹–Cys¹⁴² disulfide bond persists in the bound state of the trans isomer.

Slow exchange-related motions were also detected for Phe¹³⁷, Ile¹³⁸, and Lys¹⁴⁰ at pH 7.2 and 4.5, with exchange contributions “peaking” around Ile¹³⁸. While cis/trans isomerization around the central Ile¹³⁸–Pro¹³⁹ peptide bond would certainly affect this region of the backbone, this should occur on a time scale too slow to contribute to exchange broadening. Other possible exchange mechanisms which occur within a microsecond to millisecond time scale and could therefore contribute to exchange broadening include bending motions around the hinge residue, Ile¹³⁸, which affects the relative orientation of the two turns, or conformational exchange within the turns themselves. Conformational exchange in ordered turns has been proposed to cause T_2 exchange broadening in both ¹⁵N relaxation measurements (58–61) and ¹³C C α relaxation measurements (62). However, conformational exchange within the β -turns of the trans isomer seems unlikely as the configurations of these turns (a type I β -turn spanning Asp¹³⁴–Glu–Gln–Phe¹³⁷ and a type II β -turn spanning Pro¹³⁹–Lys–Gly–Cys¹⁴²) are well defined by the relative strengths of the $d_{\alpha\text{N}}(2,3)$, $d_{\text{NN}}(2,3)$, and $d_{\beta\text{N}}(2,4)$ cross-peaks (22, 32, 35). In addition, the NMR solution structures of the trans isomers of two other synthetic peptides, PAO and KB7, derived from the corresponding C-terminal receptor-binding regions of strains PAO and KB7 *P. aeruginosa* pilin, showed the same two sequential β -turns, conserved in both sequence and configuration despite limited sequence homology (35).

Bending motions around the hinge residue, Ile¹³⁸, offers a more plausible exchange mechanism. “Hinge-bending motions” between subdomains of human α -TGF have been invoked to explain ¹⁵N T_2 exchange broadening (63). Evidence for this mechanism in the PAK pilin system comes from a comparison of the NMR solution structures of the trans isomers of the PAK, PAO, and KB7 synthetic peptides. These structures show significant variation in the relative orientations of the first type I β -turn to the second type II β -turn (35), demonstrating the potential of large-scale hinge motions around residue 138 in each sequence. Since each of these peptides binds to Mab PAK-13 with similar affinity (μM ; 36), it has been suggested that hinge rotations about Ile¹³⁸ might place the two turns into the same relative alignment for binding (35). Hinge-bending motions about Ile¹³⁸ might similarly place the two turns of the trans and cis PAK pilin peptides into the same relative alignment for binding, even though the relative distance and orientation of the first to the second turn are different in each isomer. This would explain why both isomers bind with apparently equal affinity to Fab PAK-13, although their only shared structural feature is the type II β -turn spanning Pro¹³⁹–Lys–Gly–Cys¹⁴².

Possible Conformational Exchange Mechanisms in the Cis Isomer of the PAK Pilin Peptide. In the cis isomer, slow exchange-related motions were also detected for Thr¹³⁰ at both pH 7.2 and pH 4.5, which may also be associated with isomerization of chirality of the neighboring Cys¹²⁹–Cys¹⁴² disulfide bond. In support of this mechanism, a doubling of

⁶ In the ¹⁵N-edited NOESY HSQC spectrum of the trans isomer in the absence of Fab, a major cross-peak at 121.8, 9.16, 4.86 ppm and a minor cross-peak at 121.8, 9.16, 4.98 ppm is observed for Cys¹²⁹.

⁷ In the ¹⁵N-edited NOESY HSQC spectrum of the trans isomer in the presence of Fab, a major cross-peak at 122.0, 9.15, 4.86 ppm and a minor cross-peak at 122.0, 9.15, 4.92 ppm is observed for Cys¹²⁹.

the Cys¹²⁹ H α resonance was observed in the ¹⁵N-edited NOESY HSQC of the cis isomer in the absence Fab PAK-13 (32).⁸ Isomerization of the disulfide bond may also be the source of the slow motions detected for Gly¹⁴¹ at both pH 7.2 and pH 4.5, as this residue is located just inside the bridge (like Thr¹³⁰). As the type II conformation of the second turn in the cis isomer (Pro¹³⁹-Lys-Gly-Cys¹⁴²) is fairly well defined, the slow motions detected for Gly¹⁴¹ are less likely to be caused by conformational exchange within the turn. However, the slow motions detected for Asp¹³² at both pH 7.2 and pH 4.5 are undoubtedly caused by conformational exchange within the first turn (Asp¹³²-Gln-Asp-Glu¹³⁵), as it is poorly defined in the free solution structure of the cis isomer (34). Finally, slow motions detected for Phe¹³⁷ at both pH 7.2 and pH 4.5 are difficult to identify in the absence of a solution structure for the cis isomer; however, they may be related to phenyl ring flips of this residue. Ring flipping about the C β -C γ bond of tyrosine has been measured on the microsecond to millisecond time scale (64) and has been proposed as a ¹⁵N T₂ exchange broadening mechanism in BPTI (55).

Interestingly, exchange broadening is much more pronounced in the cis isomer than it is in the trans isomer. This is expected from the relative ratio of the isomers (1:4 cis:trans ratio at 5 °C) which predicts a greater sampling of higher energy conformational states in the less stable cis isomer. Indeed, the first turn in the cis isomer is much more poorly defined than the first turn in the trans isomer and may be quite conformationally heterogeneous.

Effect of pH on Conformational Exchange. A general increase in the contribution of exchange-related motions to relaxation is observed with increasing pH for both the trans and cis isomers. While this may result partly from increased rates of base-catalyzed solvent exchange, it may also indicate a "looser" structure at the higher pH, with increased rates of motion on all time scales. In this regard, model-free analysis of the trans isomer in its free state indicated slightly more disorder at pH 7.2, with internal motions of greater rate and amplitude than those observed at pH 4.5. Model-free analysis of the trans isomer in the presence of Fab indicated increased order at pH 7.2 versus pH 4.5. If these order parameters are converted into conformational entropy (65) and the total combined ΔS ($S_{\text{bound}} - S_{\text{free}}$) calculated, values of -38.7 J/(mol·K) at pH 7.2 and -6.29 J/(mol·K) at pH 4.5 are obtained. These values suggest that the PAK pilin peptide experiences a greater loss in conformational entropy upon Fab binding at pH 7.2, commensurate with its less ordered free state.

An increased loss in conformational entropy generally translates into decreased binding affinity. Yet, HSQC titration data presented for the trans isomer in a previous paper (32) suggest that the K_a is slightly greater at pH 7.2 than at pH 4.5. What, then, could account for the increased affinity of the interaction at pH 7.2? The pattern of backbone and side-chain NOE connectivities observed for the trans isomer at pH 7.2 and 4.5 is identical (22, 32), suggesting that neither the turns nor the hydrophobic pocket experience any significant change in conformation as a function of pH.

Furthermore, chemical shift perturbations observed for the trans isomer in the presence of Fab PAK-13 were almost identical at pH 7.2 versus pH 4.5 (32), suggesting that pH changes within this range do not significantly alter the peptide "binding surface" recognized by the antibody. The only residue to display specific pH-dependent chemical shift perturbation behavior in the trans isomer was Glu¹³⁵ (32), for which increased backbone ordering and a decreased exchange contribution at lower pH were observed in the relaxation studies presented here. A transient water molecule, more stably bound at pH 4.5, was proposed to be responsible for these pH-related differences in relaxation. A more stably bound water molecule at pH 4.5 might also contribute to the decreased antibody affinity observed for the lower pH if the optimal binding of the PAK pilin immunogen to Fab PAK-13 first required release of this water from Glu¹³⁵. Interestingly, studies of the effect of pH on adhesin function indicate that receptor-binding activity is very pH dependent, with almost zero activity at pH 4.5 and maximal activity at pHs greater than physiological (R. Irvin, unpublished results). Furthermore, a Glu¹³⁵ to Ala¹³⁵ mutation results in a more cross-reactive pilin peptide immunogen (66). As Glu¹³⁵ is the only residue that titrates within this range and displays specific pH-dependent relaxation and chemical shift behavior, it must play a critical role in adhesin function, modulating both specificity of the immune response and affinity for receptor.

Role of Conformational Exchange in the Induced-Fit Binding of PAK Pilin Peptide to Antibody. What is the role of conformational exchange in induced-fit binding of the PAK pilin peptide to antibody? Both the trans and cis isomers bind with apparently equal affinity to Fab PAK-13, although their only shared structural feature is the type II β -turn spanning Pro¹³⁹-Lys-Gly-Cys¹⁴². This conserved turn is well populated in the free solution state of both isomers and does not undergo significant stabilization upon Fab binding. By contrast, the first turns in the trans (Asp¹³⁴-Glu-Gln-Phe¹³⁷) and cis (Asp¹³³-Gln-Asp-Glu¹³⁵) isomers are less well populated in the free solution state but undergo significant stabilization upon Fab binding. Thus, binding of the first turn appears to involve an "induced-fit" mechanism. Interestingly, the site of the greatest conformational exchange in the trans isomer is Ile¹³⁸, a "hinge" for cis/trans isomerization (Ile¹³⁸-Pro¹³⁹) and a residue that coincidentally sits right in the middle of the two turns (Asp¹³⁴-Glu-Gln-Phe¹³⁷ and Pro¹³⁹-Lys-Gly-Cys¹⁴²). Conformational exchange around Ile¹³⁸ may thus modulate induced-fit binding of the first turn in the PAK pilin system, allowing the PAK-13 combining site to accommodate either a trans or a cis topology, even though the relative distance and orientation of the first to the second turn are different in each isomer.

Conformational exchange around Ile¹³⁸ may also modulate induced-fit binding of the first turn in the PAO and KB7 pilin systems, providing a mechanism for cross-reactivity of PAK-13 to various strains of *P. aeruginosa*. Thus, the presence of conformational exchange within the PAK pilin sequence may be the very factor that allows the generation of an anti-peptide antibody therapeutic that is capable of recognizing and binding the intact pilin protein from several different strains of *P. aeruginosa*. To this end, a detailed picture of the dynamics involved in antibody recognition of pilin immunogens is a necessary component of vaccine

⁸ In the ¹⁵N-edited NOESY HSQC spectrum of the cis isomer in the absence of Fab, a major cross-peak at 122.2, 9.02, 5.06 ppm and a minor cross-peak at 122.2, 9.02, 4.94 ppm is observed for Cys¹²⁹.

design, providing critically important information to the generation of an immune response cross-protective against a broad spectrum of *P. aeruginosa* strains.

ACKNOWLEDGMENT

The authors thank Robert Boyko and Leigh Willard for computer programming assistance. The BL21(DE3) cells were a generous gift provided by Dr. Joyce Pearlstone.

SUPPORTING INFORMATION AVAILABLE

Four tables giving ^{15}N T_1 and T_2 and heteronuclear NOE's, values of model-free parameters and R_{ex} terms, spectral density values, and ^{15}N T_2 and R_2 values for isomers of the recombinant ^{15}N -labeled PAK pilin peptide in the absence and presence of Fab PAK-13. This material is available free of charge via the Internet at <http://pubs.acs.org>.

REFERENCES

1. Rivera, M., and Nicotra, M. B. (1982) *Am. Rev. Respir. Dis.* 126, 833–836.
2. Pier, G. B. (1985) *J. Infect. Dis.* 151, 575–580.
3. Todd, T. R. J., Franklin, A., Mankinen-Irvin, P., Gurman, G., and Irvin, R. T. (1989) *Am. Rev. Respir. Dis.* 140, 1585–1589.
4. Sajjan, U., Reisman, J., Doig, P., Irvin, R. T., Forstner, G., and Forstner, J. (1991) *J. Clin. Invest.* 89, 657–665.
5. Irvin, R. T. (1993) in *Pseudomonas aeruginosa as an Opportunistic Pathogen* (Campa, M., Ed.) pp 19–42, Plenum Press, New York.
6. Paranchych, W., Sastry, P. A., Volpel, K., Loh, B. A., and Speert, D. P. (1986) *Clin. Invest. Med.* 9, 113–118.
7. Ramphal, R., Carnoy, C., Fiebre, S., Michalski, J.-C., Houdret, N., Lamblin, G., Strecker, G., and Roussel, P. (1991) *Infect. Immun.* 59, 700–704.
8. Doig, P., Smith, N. R., Todd, T., and Irvin, R. T. (1987) *Infect. Immun.* 55, 1517–1522.
9. Doig, P., Todd, T., Sastry, P. A., Lee, K. K., Hodges, R. S., Paranchych, W., and Irvin, R. T. (1988) *Infect. Immun.* 56, 1641–1646.
10. Doig, P., Sastry, P. A., Hodges, R. S., Lee, K. K., Paranchych, W., and Irvin, R. T. (1990) *Infect. Immun.* 58, 124–130.
11. Irvin, R. T., Doig, P., Lee, K. K., Sastry, P. A., Paranchych, W., Todd, T., and Hodges, R. S. (1989) *Infect. Immun.* 57, 3720–3726.
12. Lee, K. K., Doig, P., Irvin, R. T., Paranchych, W., and Hodges, R. S. (1989) *Mol. Microbiol.* 3, 1493–1499.
13. Lee, K. K., Sheth, H. B., Wong, W. Y., Sherburne, R., Paranchych, W., Hodges, R. S., Lingwood, C. A., Krivan, H., and Irvin, R. T. (1994) *Mol. Microbiol.* 11, 705–713.
14. Krivan, H. C., Ginsburg, V., and Roberts, D. D. (1988) *Arch. Biochem. Biophys.* 260, 493–496.
15. Krivan, H. C., Roberts, D. D., and Ginsburg, V. (1988) *Proc. Natl. Acad. Sci. U.S.A.* 85, 6157–6161.
16. Baker, N., Hansson, G. C., Leffler, H., Riise, G., and Svanbord-Eden, C. (1990) *Infect. Immun.* 58, 2361–2366.
17. Ramphal, R., Sadoff, J. C., Pyle, M., and Silipigni, J. D. (1984) *Infect. Immun.* 44, 38–40.
18. Sheth, H. B., Lee, K. K., Wong, W. Y., Srivastava, G., Hindsgaul, O., Hodges, R. S., Paranchych, W., and Irvin, R. T. (1994) *Mol. Microbiol.* 11, 715–723.
19. Lee, K. K., Paranchych, W., and Hodges, R. S. (1990) *Infect. Immun.* 58, 2727–2732.
20. Lee, K. K., Yu, L., Macdonald, D. L., Paranchych, W., Hodges, R. S., and Irvin, R. T. (1996) *Can. J. Microbiol.* 42, 479–486.
21. Yu, L., Lee, K. K., Paranchych, W., Hodges, R. S., and Irvin, R. T. (1996) *Mol. Microbiol.* 19, 1107–1116.
22. Campbell, A. P., Wong, W. Y., Houston, M. E., Jr., Schweizer, F., Cachia, P. J., Irvin, R. T., Hindsgaul, O., Hodges, R. S., and Sykes, B. D. (1997) *J. Mol. Biol.* 267, 382–402.
23. McInnes, C., Kay, C. M., Hodges, R. S., and Sykes, B. D. (1994) *Biopolymers* 34, 1221–1230.
24. Suh, J.-Y., Spyropoulos, L., Keizer, D. W., Irvin, R. T., and Sykes, B. D. (2001) *Biochemistry* 40, 3985–3995.
25. Keizer, D. W., Slupsky, C. M., Kalisiak, M., Campbell, A. P., Crump, M., Sastry, P. A., Hazes, B., Irvin, R. T., and Sykes, B. D. (2001) *J. Biol. Chem.* 276, 24186–24193.
26. Campbell, A. P., Spyropoulos, L., Irvin, R. T., and Sykes, B. D. (2000) *J. Biomol. NMR* 17, 239–255.
27. Lipari, G., and Szabo, A. (1982) *J. Am. Chem. Soc.* 104, 4546–4559.
28. Lipari, G., and Szabo, A. (1982) *J. Am. Chem. Soc.* 104, 4559–4570.
29. Farrow, N. A., Zhang, O., Szabo, A., Torchia, D. A., and Kay, L. E. (1995) *J. Biomol. NMR* 6, 153–162.
30. Carr, P. A., Erickson, H. P., and Palmer, A. G. (1997) *Structure* 5, 949–959.
31. Gao, G., Semenchenko, V., Arumugam, S., and van Doren, S. R. (2000) *J. Mol. Biol.* 301, 537–552.
32. Campbell, A. P., Spyropoulos, L., Wong, W. Y., Irvin, R. T., and Sykes, B. D. (2000) *Biochemistry* 39, 14847–14864.
33. Tripet, B., Yu, L., Bautista, D. L., Wong, W. Y., Irvin, R. T., and Hodges, R. S. (1996) *Protein Eng.* 9, 1029–1042.
34. Campbell, A. P., Bautista, D. L., Tripet, B., Irvin, R. T., Hodges, R. S., and Sykes, B. D. (1997) *Biochemistry* 36, 12791–12801.
35. Campbell, A. P., McInnes, C., Hodges, R. S., and Sykes, B. D. (1995) *Biochemistry* 34, 16255–16268.
36. Sheth, H. B., Glasier, L. M. G., Ellert, N. W., Cachia, P., Kohn, W., Lee, K. K., Paranchych, W., Hodges, R. S., and Irvin, R. T. (1995) *Biomed. Pept., Proteins, Nucleic Acids* 1, 141–148.
37. Wong, W. Y., Irvin, R. T., Paranchych, W., and Hodges, R. S. (1992) *Protein Sci.* 1, 1308–1318.
38. Nieto, A., Gaya, A., Jansa, M., Moreno, C., and Vives, J. (1984) *Mol. Immunol.* 21, 537–543.
39. Kay, L. E., Keifer, P., and Saarinen, T. (1992) *J. Am. Chem. Soc.* 114, 10663–10665.
40. Muhandiram, D. R., and Kay, L. E. (1994) *J. Magn. Reson. B103*, 203–216.
41. Farrow, N. A., Muhandiram, R., Singer, A. U., Pascal, S. M., Kay, C. M., Gish, G., Shoelson, S. E., Pawson, R., Forman-Kay, J. D., and Kay, L. E. (1994) *Biochemistry* 33, 5984–6003.
42. Shaka, A. J., Keeler, J., Frenkiel, T., and Freeman, R. (1983) *J. Magn. Reson.* 52, 335–338.
43. Loria, J. P., Rance, M., and Palmer, A. G. (1999) *J. Am. Chem. Soc.* 121, 2331–2332.
44. Shaka, A. J., Barker, P. B., and Freeman, R. (1985) *J. Magn. Reson.* 64, 547–552.
45. Delaglio, F., Grzesiek, S., Vuister, G. W., Zhu, G., Pfeifer, J., and Bax, A. (1995) *J. Biomol. NMR* 6, 277–293.
46. Garrett, D. S., Powers, R., Gronenborn, A. M., and Clore, G. M. (1991) *J. Magn. Reson.* 95, 214–220.
47. Lian, L. Y., Barsukov, I. L., Sutcliffe, M. J., Sze, K. H., and Roberts, G. C. K. (1994) *Methods Enzymol.* 239, 657–700.
48. Roder, H. (1989) *Methods Enzymol.* 239, 446–473.
49. Thanki, N., Umrana, Y., Thornton, J. M., and Goodfellow, J. M. (1991) *J. Mol. Biol.* 221, 669–691.
50. Clore, G. M., Driscoll, P. C., Wingfield, P. T., and Gronenborn, A. M. (1990) *Biochemistry* 29, 7387–7401.
51. Clore, G. M., Szabo, A., Bax, A., Kay, L. E., Driscoll, P. C., and Gronenborn, A. M. (1990) *J. Am. Chem. Soc.* 112, 4989–4991.
52. Peng, J. W., and Wagner, G. (1992) *Biochemistry* 31, 8571–8586.
53. Peng, J. W., and Wagner, G. (1992) *J. Magn. Reson.* 98, 308–332.
54. Davis, J. H., and Agard, D. A. (1998) *Biochemistry* 37, 7696–7707.
55. Otting, G., Liepinsch, E., and Wüthrich, K. (1993) *Biochemistry* 32, 3571–3582.
56. Sørensen, M. D., Bjørn, S., Norris, K., Olsen, O., Petersen, L., James, T. L., and Led, J. J. (1997) *Biochemistry* 36, 10439–10450.
57. Atkinson, R. A., Kieffer, B., Dejaegere, A., Sirockin, F., and Lefèvre, J.-F. (2000) *Biochemistry* 39, 3908–3919.
58. Nicholson, L. K., Yamazaki, T., Torchia, D. A., Grzesiek, S., Bax, A., Stahl, S. J., Kaufman, J. D., Wingfield, P. T., Lam, P. Y., Jadhav, P. K., et al. (1995) *Nat. Struct. Biol.* 2, 274–280.
59. Kontaxis, G., Konrat, R., Krautler, B., Weiskirchen, T., and Bister, K. (1998) *Biochemistry* 37, 7127–7134.
60. Barbar, E., Hare, M., Daragan, V., Barany, G., and Woodward, C. (1998) *Biochemistry* 37, 7822–7833.
61. LiWang, A. C., Cao, J. J., Zheng, H., Lu, Z., Peiper, S. C., and LiWang, P. J. (1999) *Biochemistry* 38, 442–453.
62. Beglova, N., LeSauter, L., Ekiel, I., Saragovi, H. U., and Gehring, K. (1998) *J. Biol. Chem.* 273, 23652–23658.

63. Li, Y. C., and Montelione, G. T. (1995) *Biochemistry* 34, 2408–2423.
64. Nall, B. T., and Zuniga, E. H. (1990) *Biochemistry* 29, 7576–7584.
65. Yang, D., and Kay, L. E. (1996) *J. Mol. Biol.* 263, 369–382.
66. Cachia, P. J., Hodgins, R. R., Wong, W. Y., Irvin, R. T., and Hodges, R. S. (1998) *J. Pept. Res.* 52, 289–299.

BI030102C